THE JOURNAL OF BIOLOGICAL CHEMISTRY VOL. 283, NO. 19, pp. 13330–13340, May 9, 2008

Biosynthetic Exchange of Bromide for Chloride and Strontium for Calcium in the Photosystem II Oxygen-evolving Enzymes*[S]

Received for publication, December 31, 2007, and in revised form, February 28, 2008 Published, JBC Papers in Press, March 10, 2008, DOI 10.1074/jbc.M710583200

Naoko Ishida[‡1], **Miwa Sugiura**[§], **Fabrice Rappaport**[¶], **Thanh-Lan Lai**[‡], **A. William Rutherford**[‡], **and Alain Boussac**[‡2]

From the [‡]*Institut de Biologie et Technologie de Saclay, URA CNRS 2096, Commissariat à l'Energie Atomique Saclay, 91191 Gif-sur-Yvette, France, the* [§]*Department of Plant Biosciences, School of Life and Environmental Sciences, Osaka Prefecture University, 1-1 Gakuen-cho, Naka-ku, Sakai, Osaka 599-8531, Japan, and the* [¶]*Institut de Biologie Physico-Chimique, Université Pierre et Marie Curie/CNRS UMR 7141, 13 rue Pierre et Marie Curie, 75005 Paris, France*

The active site for water oxidation in photosystem II goes through five sequential oxidation states (S_0 to S_4) before O_2 is evolved. It consists of a Mn_4Ca cluster close to a redox-active tyrosine residue (Tyr_Z). Cl^- is also required for enzyme activity. To study the role of Ca^{2+} and Cl^- in PSII, these ions were biosynthetically substituted by Sr^{2+} and Br^-, respectively, in the thermophilic cyanobacterium *Thermosynechococcus elongatus*. Irrespective of the combination of the non-native ions used (Ca/Br, Sr/Cl, Sr/Br), the enzyme could be isolated in a state that was fully intact but kinetically limited. The electron transfer steps affected by the exchanges were identified and then investigated by using time-resolved UV-visible absorption spectroscopy, time-resolved O_2 polarography, and thermoluminescence spectroscopy. The effect of the Ca^{2+}/Sr^{2+} and Cl^-/Br^- exchanges was additive, and the magnitude of the effect varied in the following order: Ca/Cl < Ca/Br < Sr/Cl < Sr/Br. In all cases, the rate of O_2 release was similar to that of the $S_3Tyr_Z^{\cdot}$ to S_0Tyr_Z transition, with the slowest kinetics (*i.e.* the Sr/Br enzyme) being ≈6–7 slower than in the native Ca/Cl enzyme. This slowdown in the kinetics was reflected in a decrease in the free energy level of the S_3 state as manifest by thermoluminescence. These observations indicate that Cl^- is involved in the water oxidation mechanism. The possibility that Cl^- is close to the active site is discussed in terms of recent structural models.

Light-driven water oxidation by the photosystem II (PSII)[3] enzyme is responsible for the O_2 on Earth and is at the origin of the production of most of the biomass. Refined three-dimensional x-ray structures at 3.5 and 3.0 Å resolution have been obtained by using PSII isolated from the thermophilic cyanobacterium *Thermosynechococcus elongatus* (1, 2). PSII is made up of more than 20 membrane protein subunits, 35–36 chlorophyll molecules, more than 10 carotenoid molecules, several lipids, two hemes, and the cofactors involved in the electron transfer reactions (1, 2). Absorption of a photon by chlorophyll is followed by the formation of a radical pair in which the pheophytin molecule, $Pheo_{D1}$, is reduced and the accessory chlorophyll molecule, Chl_{D1}, is oxidized (3–5). The cation is then stabilized on P_{680}, a weakly coupled chlorophyll dimer (see *e.g.* Refs. 6 and 7 for energetic considerations). The pheophytin anion transfers the electron to a quinone, Q_A, which in turn reduces a second quinone, Q_B. P_{680}^+ oxidizes a tyrosine residue of the D1 polypeptide, Tyr_Z, which in turn oxidizes the Mn_4Ca cluster.

The Mn_4Ca cluster acts as a device for accumulating oxidizing equivalents and as the active site for water oxidation. During the enzyme cycle, the oxidizing side of PSII goes through five sequential redox states, denoted as S_n, where n varies from 0 to 4 upon the absorption of four photons (8). Upon formation of the S_4 state, two molecules of water are rapidly oxidized, the S_0 state is regenerated, and O_2 is released.

The mechanism by which water is oxidized and O_2 produced is still largely unknown (9–17). The geometry and ligand environment of the Mn_4Ca cluster in the crystal structure is not clearly defined because the x-ray beam reduces the native high valence manganese cluster back to the Mn^{II} state (18, 19). The transition from S_4 (or $S_3Tyr_Z^{\cdot}$, which is kinetically indistinguishable) to S_0 probably involves several reaction intermediates. These have largely escaped detection for the following reasons: 1) the rate constant of this transition is rapid ($t_{1/2} \approx 1$ ms); 2) the reduction of $Tyr_Z^{\cdot}$ is the limiting step for water oxidation in the native enzyme; and 3) experimental methods for trapping potential intermediate states are lacking (see Refs. 20 and 21 for a recent elegant thermodynamic approach). One strategy that could allow intermediates to be detected is to modify the enzyme, maintaining its capacity for turnover but impairing its kinetics. A change in the rate-limiting step could

* This work was supported in part by the Japan Society for the Promotion of Science (JSPS) and the CNRS under the Japan-France Research Cooperative Program and Solar-H, a Space Technologies Research Program from the European Community. The costs of publication of this article were defrayed in part by the payment of page charges. This article must therefore be hereby marked "*advertisement*" in accordance with 18 U.S.C. Section 1734 solely to indicate this fact.

[S] The on-line version of this article (available at http://www.jbc.org) contains supplemental Equations 1–6, Figs. S1–S6, and Table ST1.

[1] Supported in part by the Bio-Hydrogen Program of the Commissariat à l'Energie Atomique.

[2] To whom correspondence should be addressed. Tel.: 33-1-69-08-72-06; E-mail: alain.boussac@cea.fr.

[3] The abbreviations used are: PSII, photosystem II; P_{680}, primary electron donor; Chl, chlorophyll; DCBQ, 2,6-dichloro-*p*-benzoquinone; PPBQ, phenyl-*p*-benzoquinone; EXAFS, extended X-ray absorption fine structure; Nd:YAG, neodymium-yttrium aluminum garnet; Pheo, pheophytin; Q_A and Q_B, primary and secondary quinone acceptors; MES, 4-morpholineethanesulfonic acid; Tricine, *N*-[2-hydroxy-1,1-bis(hydroxymethyl)ethyl]glycine.

allow one or more intermediates to become detectable. Recently (22), we have shown that growing the thermophilic cyanobacterium *T. elongatus* in the presence of Sr^{2+} instead of Ca^{2+} resulted in the exchange of Ca^{2+} by Sr^{2+}, and this produced a significant slowdown of the oxygen evolution rate. Among all of the cations tested, only Sr^{2+} can substitute for Ca^{2+} (23–26).

The effects of Ca^{2+}/Sr^{2+} exchange have been studied by EPR (22, 27–29), Fourier transform infrared spectroscopy (30–32), EXAFS spectroscopy (33, 34), mass spectrometry experiments monitoring the water substrate exchange rates (35), and time-resolved UV-visible spectroscopy (22). Ca^{2+}/Sr^{2+} exchange has a slight effect on the geometry of the manganese cluster as detected by EPR (27, 28). The kinetics of O_2 release and the $S_3Tyr_Z^{\bullet}$ to S_0Tyr_Z transition are slowed down to the same extent (22). The affinity of the slowest exchangeable water substrate molecule bound in the S_3 state is decreased (35). These studies indicate the involvement of Ca^{2+} (or Sr^{2+}) in the catalytic cycle (10, 36, 37).

When Ca^{2+} is removed from its site, manganese oxidation can still take place, allowing the formation of the S_2 state, but in the following step, the normal S_3 state is not formed. Instead, an alternative, abnormally stable form appears to be induced in which the Mn_4 cluster is in the same redox state as it was in S_2 state but in magnetic interaction with a radical (spin = 1/2) (38), likely $Tyr_Z^{\bullet}$ (39, 40), giving rise to a characteristic EPR signal that is known as the split signal.

Choride is also an essential ion for PSII activity (24, 26, 41–53). In plant PSII, removal of Cl^- inhibits oxygen evolution and perturbs the Mn_4 cluster to a variable extent depending on the precise Cl^--depletion method used (24, 26, 46). The removal of Cl^- by incubation in Cl^--free buffer increased the proportion of the Mn_4 cluster in the high-spin state (g = 4 EPR signal), but the enzyme continues to work at a reduced rate (46). When Cl^- is removed by a high pH shock, the high-spin state is formed, and the S-state cycle is blocked after S_2 formation in the majority of centers, whereas treatment with SO_4^{2-} inhibits the enzyme but allows radical ($Tyr_Z^{\bullet}$) formation in the presence of S_2, giving rise to the split EPR signal, at least in a fraction of the centers (46, 47, 53, 54). In the SO_4^{2-}-treated enzyme the electron donation rate from Tyr_Z to P_{680}^+ is not greatly affected on the first two flashes (47), but Cl^- is required to progress through the S_2 to S_3 (46, 47, 50) and S_3 to S_0 transitions (50).

When the first PSII structural models from crystallography appeared, the resolution was not good enough to detect the Ca^{2+} ion (55, 56), and the question arose whether Ca^{2+} really was intimately associated with the Mn_4 cluster in cyanobacteria as was thought to be the case in plants. This prompted us to develop a method for biosynthetic Ca^{2+}/Sr^{2+} exchange in *T. elongatus* (22). We showed that there is one Sr^{2+} per PSII in fully active cyanobacterial PSII (22). At the same time, a structure with 3.5 Å resolution was reported in which a Ca^{2+} ion in close interaction with the Mn_4 cluster was identified based on anomalous diffraction data (1). Recently, x-ray crystallography and EXAFS spectroscopy using the Sr^{2+}-containing enzyme confirmed that Sr^{2+} was associated with the Mn_4 cluster and was located in a position similar to that of Ca^{2+} (34, 57).

The situation for chloride is less clear. No chloride ions are defined in the current three-dimensional structural models of the enzyme (1, 2). This is partly because the resolution is insufficient but also because the structure of the cluster is perturbed by the x-ray beam, which reduces the high valence manganese cluster to the Mn^{II} state (18, 19). The role and location of chloride as a cofactor in PSII from cyanobacteria thus remain open. For this reason, Cl^-/Br^- exchange experiments are potentially interesting.

Previously reported Cl^-/Br^- exchange studies were done in chloride-depleted PSII. Depending on the Cl^--depletion procedure (*e.g.* sulfate treatment at high pH *versus* extrinsic polypeptide depletion), the Br^- reconstitution may have different effects. These differences can be explained by the presence of more than one chloride-binding site in PSII, the activity of which would depend on the binding of chloride to a high affinity site; and this activity could be modulated by the binding of another chloride to a low affinity binding site (46, 48). An alternative interpretation has been suggested, namely that many of the effects induced by Cl^- depletion are depletion-induced artifacts and that there is a single Cl^--binding site that has only an indirect effect on enzyme function. Indeed, in this interpretation Cl^- is not considered necessary for enzyme activity (51, 52).

As in the case of Ca^{2+}/Sr^{2+}, the biosynthetic substitution of Br^- for Cl^- could provide a "bromide phenotype" that does not suffer from the ambiguities associated with biochemical exchange procedures. The study of the bromide exchanged PSII could yield evidence for the involvement of Cl^- in the water-splitting process and provide new insights on the role of chloride in the water oxidation mechanism.

Here we present the results of this biosynthetic Cl^-/Br^- replacement study using *T. elongatus* with either Ca^{2+} or Sr^{2+} in the active site. Fully intact PSII preparations containing Ca/Cl, Ca/Br, Sr/Cl, and Sr/Br were analyzed using a combination of spectroscopic and enzymological studies.

EXPERIMENTAL PROCEDURES

Culture of the Cells and Purification of Thylakoids and PSII—Thylakoids, and thence PSII, were purified from a *T. elongatus* strain that had a His_6 tag on the CP43 subunit (58) and in which the *psbA*$_1$ and *psbA*$_2$ genes were deleted (WT*) (59). The D1 protein in PSII can potentially be encoded by three genes, *psbA*$_1$, *psbA*$_2$, and *psbA*$_3$, each differing slightly. Because in this WT* *T. elongatus* only the *psbA*$_3$ gene is present, the enzyme is not affected by the possible heterogeneity in D1 that would result from the expression of more than one of the three *psbA* genes. Such a situation could occur, for example, because of regulatory mechanisms triggered when changing light intensity during batch culture (60).

The WT* cells were grown in 1 liter of culture medium (58) in 3-liter Erlenmeyer flasks in a rotary shaker with a CO_2-enriched atmosphere at 45 °C under continuous light (80 μmol of photons·m^{-2}·s^{-1}). The culture medium was supplemented with either 0.8 mM CaX_2 or SrX_2 (X was either bromide or chloride depending on the experiments). The grade of the chemicals used was ≥99.999% for $CaBr_2$, $SrCl_2$, and $SrBr_2$ and ≥99.99% for $CaCl_2$. The chloride content was ≤0.001% in glyc-

TABLE 1

PSII	Activity[a]	α[b]	S_0/S_1[b]	$t_{1/2}$[c]			TL in S_3[e]
				$S_1TyrZ^{\cdot}$ to S_2TyrZ	$S_3Tyr_Z^{\cdot}$ to $(S_3Tyr_Z^{\cdot})'$	$(S_3Tyr_Z^{\cdot})'$ to S_0[d]	
	μmol O_2/mg Chl·h	*%*	*%/%*	*μs*	*μs*	*ms*	*°C*
CaCl	5000–6000	9	0/100	≈50	115	1.1	48
CaBr	3200–3600	9	10/90	≈100	140	2.1	50
SrCl	1800–2600	9	9/91	≈150	210	4.8	52
SrBr	1500–2000	8	23/77	≈400–500	230	7.2	56

[a] Measured under continuation illumination.
[b] Miss parameter calculated from the oscillating patterns at 292 nm.
[c] Measured at 292 nm.
[d] The kinetics after the third flash were fitted according to the equation: $A(t) = (A(0)k1/(k2 - k1)) \times (e^{-k1\cdot t} - e^{-k2\cdot t}) + A(0)\cdot e^{-k1\cdot t}$ + offset, in which $A(0)$ is the calculated absorption at time $t = 0$; *i.e.* the absorption 10 μs after the third flash (the first point of the kinetics) and the offset is the calculated absorption 300 ms after the flash (the last point of the kinetics). See supplemental data for additional comments.
[e] Temperature peak position of the thermoluminescence glow curves from the $S_3Q_B^-$ charge recombination.

erol, ≤0.02% in betaine, and ≤0.005% in MES. In the culture medium and before the addition of the CaX_2 or SrX_2 salts, the Ca^{2+} contamination was measured by ICP (22) to be less than 1.5 μM. The Cl^- contamination can be estimated from the specifications given by the suppliers of the chemicals to be ≤40 μM (essentially from the Tricine buffer).

Thylakoids and PSII were prepared as described earlier (61) with the exception that no polyethylene glycol was used to concentrate the samples. Instead, the samples were concentrated by using Amicon Ultra-15 concentrator devices (Millipore) with a 100-kDa cut-off. Routinely, the total amount of Chl after the breaking of the cells was ≈180 mg, and the yield after PSII purification in terms of Chl amounts was ≈4–5%. Thylakoids and PSII were stored in liquid nitrogen at a concentration of about 1.5–2 mg Chl/ml in a medium containing 10% glycerol, 1 M betaine, 15 mM CaX_2, 15 mM MgX_2, and 40 mM MES, pH 6.5 (pH adjusted with NaOH), until they were used.

Oxygen Evolution under Continuous Light—Oxygen evolution of PSII under continuous light was measured at 25 °C by polarography using a Clark-type oxygen electrode (Hansatech) with saturating white light at a Chl concentration of 5 μg of $Chl\cdot ml^{-1}$ in the media described above. A total of 0.5 mM DCBQ (2,6-dichloro-*p*-benzoquinone, dissolved in dimethyl sulfoxide) was added as an electron acceptor. The betaine, DCBQ, and Q_B react in the time range of minutes in the presence of O_2. For that reason, measurements of PSII activity were done at ≤1 min after the addition of DCBQ.

Flash-induced Oxygen Evolution—Oxygen evolution under flashing light was measured with a laboratory-made rate electrode (22). Two combinations of electrodes were used: either Pt/Ag/AgCl or Pt/Ag/AgBr, depending on the conditions. The Ag/AgCl and Ag/AgBr electrodes were prepared by using 1–2 M HCl or HBr acids, respectively. Thylakoids were used at 1.2 mg $Chl\cdot ml^{-1}$. Typically, 25 μl of a thylakoid suspension was put onto the platinum electrode. The volume of the circulating medium was ≈250 ml and contained 10% glycerol, 1 M betaine, 15 mM CaX_2, 15 mM MgX_2, 50 mM K*X*, and 40 mM MES, pH 6.5 (pH adjusted with NaOH). Illumination was done with a xenon flash (PerkinElmer Optoelectronics). The intensity of the flash was adjusted so that the light intensity was saturating (*i.e.* the miss parameter was minimum). Measurements were done at room temperature (20–25 °C). The amplified amperometric signal resulting from the flash-induced oxygen evolution was recorded with a numerical oscilloscope.

UV-visible Absorption Change Spectroscopy—Absorption changes were measured with a laboratory-built spectrophotometer where the absorption changes were sampled at discrete times by short flashes (62). These flashes were provided by a neodymium-yttrium aluminum garnet (Nd:YAG) pumped (355 nm) optical parametric oscillator, which produces monochromatic flashes (1 nm full-width at half-maximum) with a duration of 6 ns. Excitation at 685 nm was provided by a dye laser pumped by a frequency-doubled Nd:YAG laser. The path length of the cell was 2.5 mm. PSII was used at 25 μg of $Chl\cdot ml^{-1}$ in 10% glycerol, 1 M betaine, 15 mM CaX_2, 15 mM MgX_2, and 40 mM MES, pH 6.5 (pH adjusted with NaOH). After dark adaptation for 1 h at room temperature (20–22 °C), 0.1 mM PPBQ dissolved in dimethyl sulfoxide was added as an electron acceptor. PPBQ was used here instead of DCBQ because of the length of the experiment (see above).

Thermoluminescence Experiments—Thermoluminescence glow curves were measured with a laboratory-built apparatus (63). PSII samples at 10 μg $Chl\cdot ml^{-1}$ were first dark-adapted at room temperature for 1 h. Illumination was done by using saturating xenon flashes (PerkinElmer Optoelectronics) at 5 °C. Then the samples were frozen to −10 °C in 5 s. After an additional 5 s at −10 °C, the frozen samples were heated at a constant rate (0.33 °C/s). From the lifetime of the S_2 and S_3 states at room temperature (22), these states can be considered as stable under these experimental conditions before the heating process. Analysis of the data was done as described previously (63–65).

EPR Spectroscopy—cw-EPR spectra were recorded using a standard ER 4102 (Bruker) X-band resonator with a Bruker Elexsys 500 X-band spectrometer equipped with an Oxford Instruments cryostat (ESR 900). Flash illumination at room temperature was provided by a Nd:YAG laser (532 nm, 550 mJ, 8-ns Spectra Physics GCR-230-10). PSII samples at ≈1 mg of $Chl\cdot ml^{-1}$ were loaded in the dark into quartz EPR tubes and further dark-adapted for 1 h at room temperature. Then, the samples were in some cases synchronized in the S_1 state with one pre-flash (66). After another dark period of 1 h at room temperature, 0.5 mM PPBQ was added (the final concentration of dimethyl sulfoxide was ≈2%). The samples were frozen in the dark to 198 K and then transferred to 77 K. Prior to the measurements the samples were degassed at 198 K as described previously (29).

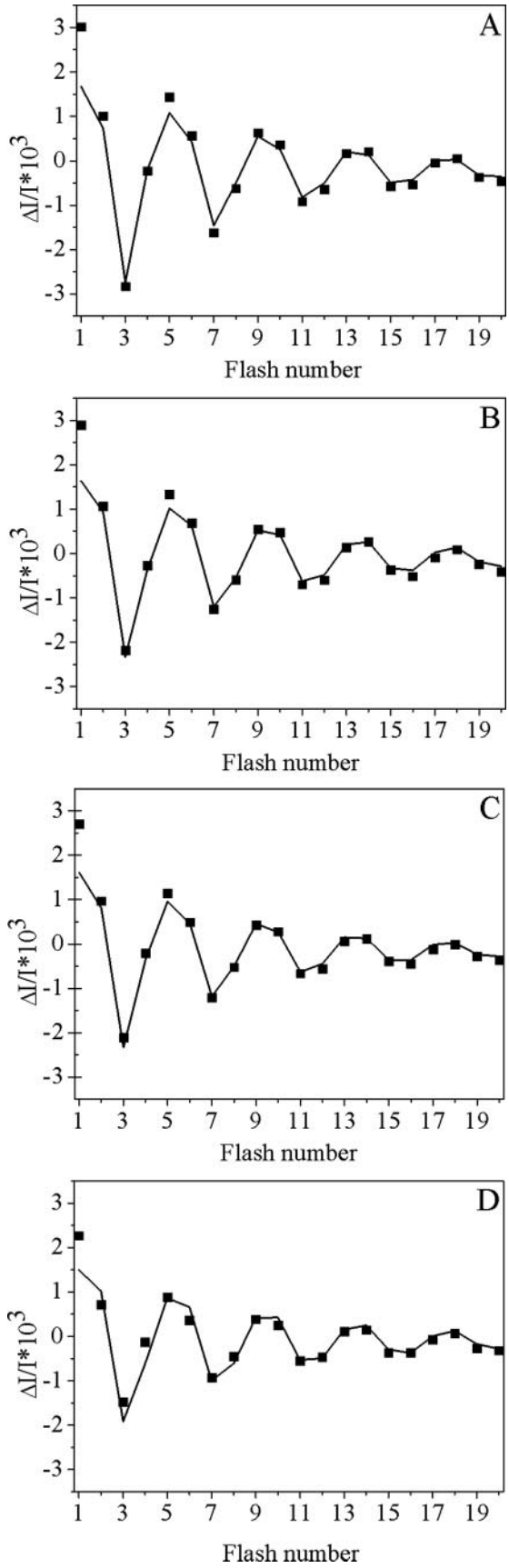

FIGURE 1. **Sequence of the amplitude of the absorption changes at 292 nm.** The measurements were done during a series of saturating flashes (spaced 400 ms apart) given to CaCl-PSII (*A*), CaBr-PSII (*B*), SrCl-PSII (*C*), and SrBr-PSII (*D*). The samples (Chl = 25 μg/ml) were dark-adapted for 1 h at room temperature before the addition of 100 μM PPBQ. The measurements were done 300 ms after each flash. The *symbols* correspond to the experimental points and the *lines* to the fit of the data.

Analysis of the data was done using Excel (Microsoft), Mathcad 14 (Parametric Technology Corp.), and Origin 7.5 (OriginLab Corp.).

RESULTS

O_2 Evolution under Continuous Illumination—We have shown previously that PSII purified from *T. elongatus* cells grown in the presence of Sr^{2+} salts incorporated one Sr^{2+} ion per four manganese ions (22), and that replaces the Ca^{2+} in the active site of PSII (22, 34, 57). Without any further biochemical treatments, this Sr^{2+} ion was not exchangeable for Ca^{2+} ions when present in the medium (22). In contrast, the exchangeability of Cl^- in the chloride site(s) is still being discussed in the literature. Therefore, to avoid any potential Br^-/Cl^- (or Cl^-/Br^-) exchange during the purification procedures, the thylakoids and the isolated PSII preparations were purified in media containing either (i) $CaCl_2$ and $MgCl_2$ for the cells grown in the presence of chloride salts or (ii) $CaBr_2$ and $MgBr_2$ for the cells grown in the presence of bromide salts. PSII (and thylakoids) purified under these different conditions are designated CaCl-PSII (CaCl-thylakoids), CaBr-PSII (CaBr-thylakoids), SrCl-PSII (SrCl-thylakoids), and SrBr-PSII (SrBr-thylakoids). The O_2 evolution activities of these four different PSII types under continuous illumination and in the corresponding suspending media are shown in Table 1. In all of these cases, the exchange of Ca^{2+} or/and Cl^- resulted in a decrease in the steady-state oxygen evolution rate.

Absorption Changes at 292 nm—Fig. 1 shows the amplitude of the absorption changes upon flash illumination recorded with the four PSII preparations. Measurements were done using a Joliot-type spectrophotometer at 292 nm (67, 68) and in the hundreds of ms time range, *i.e.* after the reduction of $Tyr_Z^{\bullet}$ by the $Mn_4Ca(Sr)$ cluster was complete. This wavelength corresponds to an isosbestic point for $PPBQ^{\bullet-}$/PPBQ, the added electron acceptor (not shown), and is in a spectral region where the absorption of the Mn_4Ca cluster depends on the S-states (68). The oscillating pattern with a period of four is clearly observed for all four types of PSII preparations irrespective of their Ca^{2+}/Sr^{2+} and Cl^-/Br^- status.

Using the formula developed by Lavorel (69) and the oscillating patterns shown in Fig. 1, the miss (α) and double-hit (β) parameters could be calculated. In this experiment, the double-hit parameter, 4–5%, was due to a small actinic effect of the measuring beam rather than an intrinsic property of PSII. The miss parameter was independent of the nature of ion present (Table 1) as already observed in CaCl-PSII and SrCl-PSII (22). Using the method developed by Lavergne (68), the four sets of data in Fig. 1 were fitted simultaneously as described previously (22, 61). Each of the three different differential extinction coefficients, $\Delta\epsilon_0$, $\Delta\epsilon_1$, $\Delta\epsilon_2$, corresponding to the S_0 to S_1, S_1 to S_2, and S_2 to S_3 transitions, respectively, was kept fixed for the four types of PSII. The S_0/S_1 ratio was allowed to vary for each type of sample (Table 1).

The $\Delta\epsilon_0$ (0.70 10^{-3}), $\Delta\epsilon_1$ (1.98 10^{-3}), and $\Delta\epsilon_2$ (1.33 10^{-3}) values found here are in good agreement with those found earlier at this wavelength (22, 61, 68). The reasonably good fits obtained when using the same set of $\Delta\epsilon_i$ for various PSII samples indicate that: (i) the Sr^{2+} and/or Br^- substitutions did not significantly modify the absorption of the Mn_4 cluster, at least at 292 nm; and (ii) there were no nonfunctional centers in the CaBr-, SrCl-, and SrBr-PSII. EPR measurements without any pre-flash illumination showed no indication for an increased proportion of centers with reduced Tyr_D in the dark-adapted SrBr-PSII (not shown) (66). Therefore, the apparent higher proportion of the S_0 state in the dark-adapted SrBr-PSII (Table 1) more likely corresponds to a higher proportion of the $S_0Tyr_D^\bullet$ state rather than to a higher proportion of the S_1Tyr_D state.

The absence of any major consequences of the Sr^{2+} and/or Br^- substitution on the turnover of the S-state cycle under flashing conditions contrasts with the significant decrease in the oxygen evolution rate under steady-state conditions. This suggests that this decreased efficiency results not from a fraction of PSII centers inactive in water splitting but rather from a change in the intrinsic kinetics of at least one of the steps in the cycle.

To determine which step(s) is affected by the Cl^-/Br^- and Ca^{2+}/Sr^{2+} exchanges, we measured the absorption changes at 292 nm in the hundreds of ns to ms time range after each of the first four flashes given to dark-adapted PSII (Fig. 2). Absorption changes at this wavelength reflect the Mn_4 cluster valence changes and the Tyr_Z redox state changes occurring in the $S_1Tyr_Z^\bullet$ to S_2Tyr_Z, $S_2Tyr_Z^\bullet$ to S_3Tyr_Z, $S_3Tyr_Z^\bullet$ to S_0Tyr_Z, and $S_0Tyr_Z^\bullet$ to S_1Tyr_Z transitions (68). Fig. 2 shows that only minor absorption changes could be detected after the second flash (*panel B*) and the fourth flash (*panel D*). This means that, in all four types of the enzyme, the ΔI/I changes associated with the $Tyr_Z^\bullet S_2$ to Tyr_ZS_3 and $Tyr_Z^\bullet S_0$ to Tyr_ZS_1 were small, thus precluding the reliable kinetic analysis of the S_2 to S_3 and S_0 to S_1 transitions. On the other hand, because these two transitions only weakly contribute to the absorption changes at this wavelength, the half-times of the S_1 to S_2 and S_3 to S_0 transitions may be reliably determined from the raw data without any deconvolution procedures. The $S_1Tyr_Z^\bullet$ to S_2Tyr_Z transition (Fig. 2*A*) was slowed down from $t_{1/2} \approx 50$ μs in CaCl-PSII to $t_{1/2} \approx 400$–500 μs in SrBr-PSII with the following order for the $t_{1/2}$ values: $t_{1/2}$ in CaCl-PSII < $t_{1/2}$ in CaBr-PSII < $t_{1/2}$ in SrCl-PSII < $t_{1/2}$ in SrBr-PSII (Table 1). The small absorption change associated to the $S_1Tyr_Z^\bullet$ to S_2Tyr_Z transition did not allow us to determine whether a multiphasic process was involved.

The kinetics of the $S_3Tyr_Z^\bullet$ to S_0Tyr_Z transition in the $CaCl_2$ sample (Fig. 2*C*) was much better fitted when a lag phase was introduced (see supplemental data). Such a lag phase was observed earlier and was attributed to structural rearrangements in the $S_3Tyr_Z^\bullet$ state (67, 70–72). Therefore the four traces were fitted with a sequential model involving the transient formation of a $(S_3Tyr_Z^\bullet)'$ state (Table 1). Based on this fitting procedure, the $t_{1/2}$ of the lag phase in SrBr-PSII is double that in CaCl-PSII. In agreement with the oxygen evolution rate under continuous illumination, the kinetics of the $S_3Tyr_Z^\bullet$ to S_0Tyr_Z transition observed after the third flash (Fig. 2*C*) was

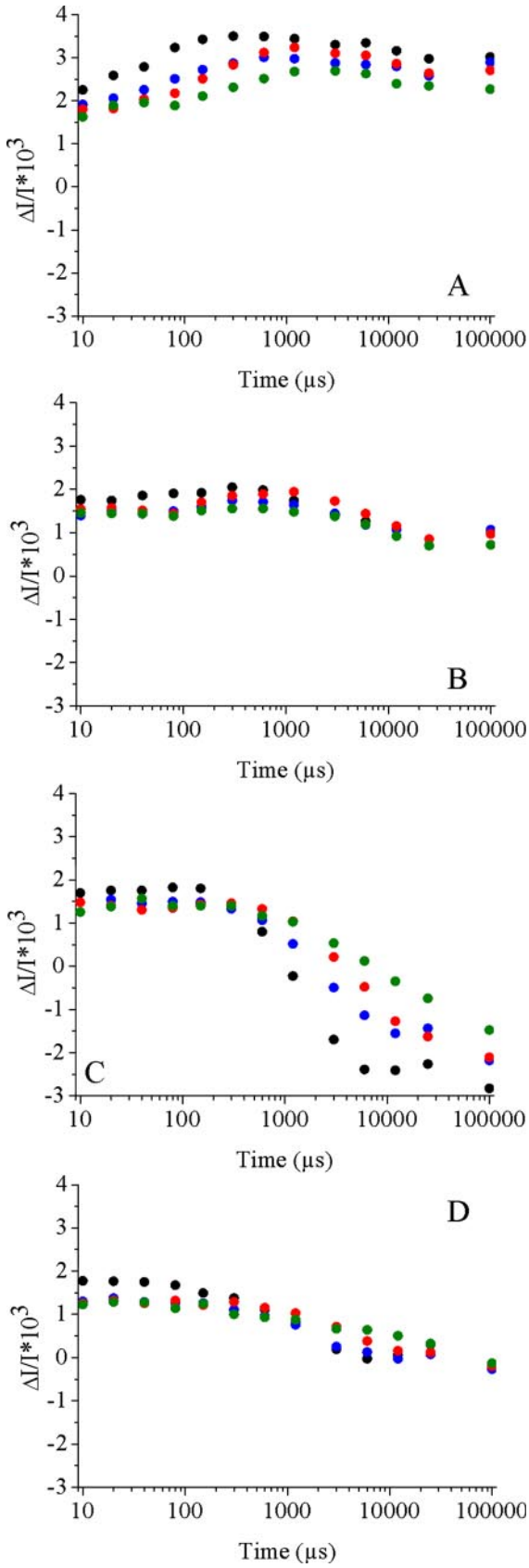

FIGURE 2. **Kinetics of the absorption changes at 292 nm after the first flash (*A*), the second flash (*B*), the third flash (*C*), and the fourth flash (*D*) given to dark-adapted CaCl-PSII (*black*), CaBr-PSII (*blue*), SrCl-PSII (*red*), and SrBr-PSII (*green*).** Other experimental conditions were similar to those in Fig. 1.

also significantly slowed down, with half-times ranging from 1.1 ms in CaCl-PSII to 7.2 ms in SrBr-PSII (Table 1).

Time-resolved O_2 Evolution—Another way to study specifically the $S_3Tyr_Z^{\bullet}$ to S_0Tyr_Z transition is to follow the O_2 release with a time-resolved polarized electrode. Because this technique requires the sedimentation of the sample on the platinum electrode, thylakoids were used instead of purified PSII. The classical electrode combination, Pt/Ag/AgCl, requires the presence of a chloride salt as an electrolytic counter anion in the circulating medium. To avoid the possible exchange of Br^- for Cl^- in the bromide-containing samples during the course of the experiment, a Pt/Ag/AgBr electrode combination with a bromide salt as an electrolytic counter anion in the circulating medium was also used as a control experiment.

Fig. 3 shows the kinetics of O_2 release in CaCl-, CaBr-, SrCl-, and SrBr-thylakoids with either a Pt/Ag/AgCl (*panel A*) or a Pt/Ag/AgBr (*panel B*) electrode combination. To get a signal with maximal amplitude, the measurements were done upon the third flash given to a dark-adapted sample. Although the chlorophyll concentration was the same for each sample, the traces shown in Fig. 3 were scaled so that the areas under the curves (the amount of evolved O_2) were identical in order to take into account the possible variations in the PSII/PSI ratio. The normalization factors were in the range of what was expected from the PSI to PSII ratio, which varied from 1.8 to 2.5 in our *T. elongatus* thylakoids (not shown) as estimated by EPR (73). Moreover, the kinetics of O_2 release were found to be similar to those observed in whole cells, which indicates that the isolation protocol had no secondary effects.

As demonstrated by Lavorel (74), the amperometric signal results from the convolution of the diffusion limited O_2 pulse produced instantaneously in a thin layer, $\Phi(t)$, with the rate constant of the $S_3Tyr_Z^{\bullet} \rightarrow S_0Tyr_Z + O_2$ reaction, k_{ox}. Thus, the ideal experimental case is that of a thylakoid monolayer. Deviating from this ideal case results in a divergence between the theoretical and experimental curves, which increases with the time after the O_2 pulse is triggered. We therefore analyzed the kinetics shown in Fig. 3 within a slightly simplified framework (see supplemental data). The O_2 diffusion time was first determined from the kinetics obtained with CaCl-thylakoids. Then, the expected traces for the four samples were calculated by using k_{ox} values equal to those of the rate constants of the $S_3Tyr_Z^{\bullet}$ to S_0Tyr_Z transition measured at 292 nm (the lag phase was neglected) (Table 1). The calculated traces resulting from such a procedure are shown in Fig. 3*C*. As mentioned above, the time resolution of the amperometric signal strongly depends on the O_2 diffusion time, which is used to calculate the function $\Phi(t)$ (k_d = 0.11 ms^{-1} in Fig. 3*C*). Although, this k_d value does not seem large enough to fully resolve the differences between the CaCl and CaBr samples, the relative $t_{1/2}$ values for both the O_2 release and the $S_3Tyr_Z^{\bullet}$ to S_0Tyr_Z transition in the four samples (Table 1) are in satisfactory agreement with those of the O_2 evolution activities measured under continuous illumination. This provides further evidence that, in these samples, the lower O_2 evolution activities arise from a kinetic limitation of the water-splitting process rather than from a fraction of inactive centers.

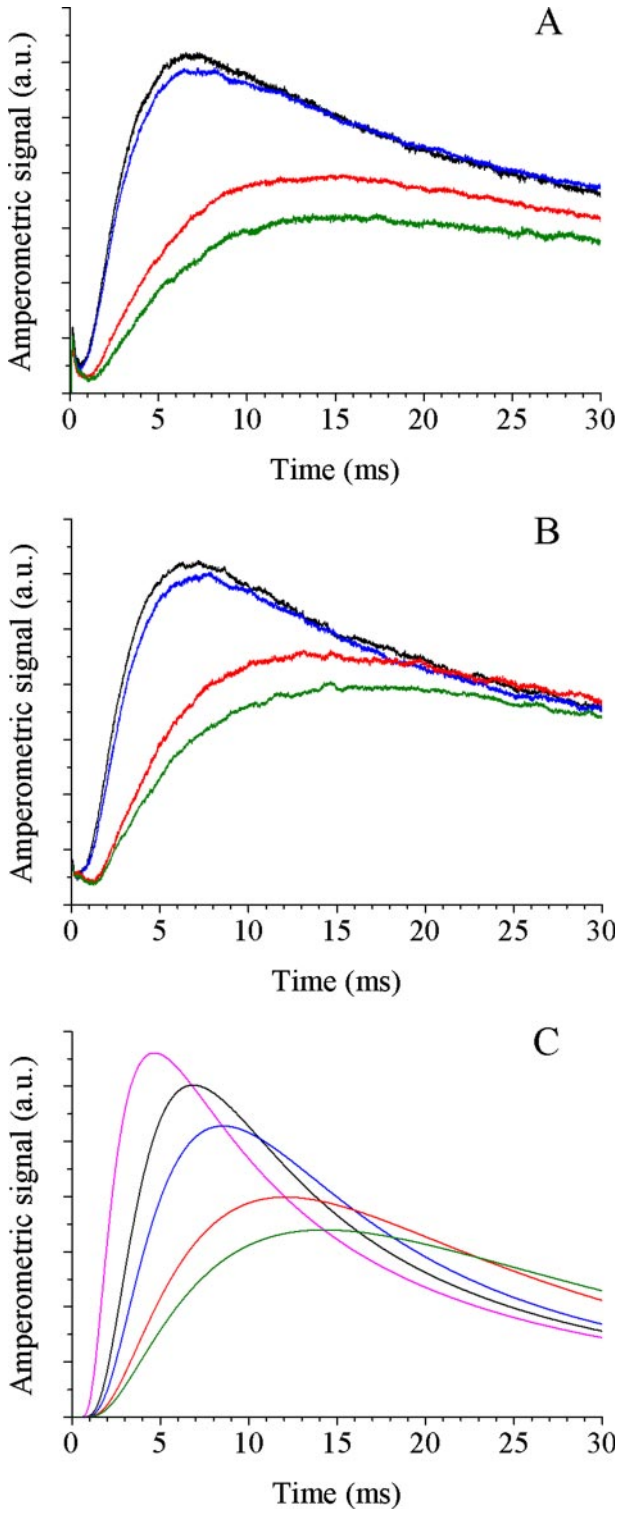

FIGURE 3. **Kinetics of the oxygen release measured after the third flash given on CaCl-thylakoids (*black*), CaBr-thylakoids (*blue*), SrCl-thylakoids (*red*), and SrBr-thylakoids (*green*).** The measurements were done with either a Pt/Ag/AgCl (*A*) or a Pt/Ag/AgBr (*B*) electrode combination. The time-resolved flash-induced oxygen evolution was measured after the third flash of a sequence of flashes spaced 400 ms apart. The samples (Chl = 1.2 mg/ml) were dark-adapted for 45 min at room temperature on the polarized bare platinum electrode prior to the illumination. *C*, expected amperometric signal in CaCl-thylakoids (*black*), CaBr-thylakoids (*blue*), SrCl-thylakoids (*red*), and SrBr-thylakoids (*green*). The *traces* were calculated by using a diffusion time value defined as indicated in the supplemental data and by using the rate constant of the $S_3Tyr_Z^{\bullet}$ to S_0Tyr_Z transition measured at 292 nm, as reported in Table 1. The violet curve is the $\Phi(t)$ function for a t_d value equal to 7 ms.

Another important conclusion, which can be drawn from a comparison of Fig. 3, *A versus B*, is that the incubation of SrBr-thylakoids in a Cl^--containing buffer and SrCl-thylakoids in a Br^--containing buffer for the 45 min required for dark adaptation of the samples had no detectable effect on the kinetics of O_2 release. Based on the volume of the samples deposited onto the platinum electrode (25 μl) and on the volume of the circulating medium (250 ml), the concentration of bromide and chloride salts can be estimated to be 6 μM and 110 mM, respectively, for the SrBr-thylakoids and *vice versa* for the SrCl-thylakoids. Since the Cl^-/Br^- exchange strongly affects the rate of O_2 release in the Sr^{2+}-containing sample, it is clear from the results shown in Fig. 3 that during the course of the experiment (≈1 h), neither Br^-/Cl^- exchange nor Cl^-/Br^- exchange occurred to a significant extent in SrBr- and SrCl-thylakoids, respectively.

As a further test of the Cl^-/Br^- and Br^-/Cl^- exchangeabilities in thylakoids, we washed the SrBr-thylakoids more extensively in the chloride-containing medium and the SrCl-thylakoids in the bromide-containing medium. The washing of these samples was done by centrifugation and resuspension (three times) until the residual amount of the contaminating halide calculated from the starting concentration was theoretically less than 0.1 μM. The overall duration of these additional washing treatments was ~3 h. After these treatments the O_2 release in SrBr-thylakoids resuspended in the chloride-containing medium and in SrCl-thylakoids resuspended in the bromide-containing medium was measured and was found to be similar to that measured in Fig. 3, *A* and *B*. This showed that, under these conditions, neither Cl^-/Br^- nor Br^-/Cl^- exchange occurred. However, when isolated PSII was incubated in the dark for 6–7 h (with a chlorophyll concentration of 25 μg/ml and a halide concentration of 60 mM as above), the measurement at 292 nm of the $S_3Tyr_Z^{\bullet}$ to S_0Tyr_Z transition rate in SrCl-PSII and SrBr-PSII showed that a Cl^-/Br^- and Br^-/Cl^- exchange had begun to occur (not shown).

Thermoluminescence and Thermodynamic Properties of the S-states—All of the kinetic results presented above strongly suggest that the redox properties of the Mn_4 cluster were modified upon Ca^{2+}/Sr^{2+} and Cl^-/Br^- exchanges. Such redox changes may be monitored by measuring the thermoluminescence glow curves (75, 76). Indeed, the amplitude and the temperature dependence of the thermolumiscence glow curve, which arises from the radiative recombination between the positive charge stored on the Mn_4 cluster and the electron stored on the quinone $Q_B^{\bullet-}$, depend in part on the redox potential of the cofactors involved in the charge recombination process, *i.e.* the redox potential of the S_{n+1}/S_n, $Tyr_Z^{\bullet}/Tyr_Z$, P_{680}^{+}/P_{680}, $Pheo_{D1}^{\bullet-}/Pheo_{D1}$, $Q_A^{\bullet-}/Q_A$, and $Q_B^{\bullet-}/Q_B$ couples (64, 65, 75–78). If we assume as a first approximation that the Ca^{2+}/Sr^{2+} and Cl^-/Br^- exchanges do not significantly modify the redox potential of the P_{680}^{+}/P_{680}, $Pheo_{D1}^{\bullet-}/Pheo_{D1}$, $Q_A^{\bullet-}/Q_A$, and $Q_B^{\bullet-}/Q_B$ couples and do not affect the proportion of reduced $Q_B^{\bullet-}$ upon dark adaptation, then the changes in the thermoluminescence glow curves are expected to reflect a change in the redox properties of the S_{n+1}/S_n couple. Fig. 4 shows such an experiment with CaCl-PSII, CaBr-PSII, SrCl-PSII, and SrBr-PSII.

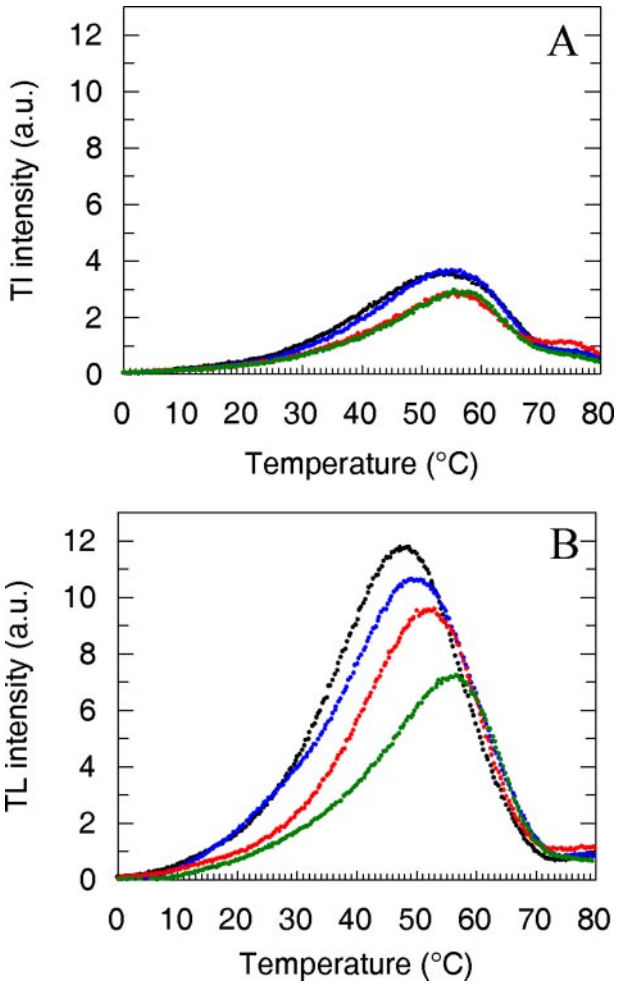

FIGURE 4. **Thermoluminescence glow curves from $S_2Q_B^{\bullet-}$ charge recombination measured after one flash (*A*) and from $S_3Q_B^{\bullet-}$ charge recombination measured after two flashes (*B*) in CaCl-PSII (*black*), CaBr-PSII (*blue*), SrCl-PSII (*red*), and SrBr-PSII (*green*).** Samples were previously dark-adapted at room temperature before being loaded into the cuvette and illuminated at 5 °C.

After one flash given to a dark-adapted sample, the glow curve originates from $S_2Q_B^{\bullet-}$ charges recombination, whereas after the second flash it originates from the $S_3Q_B^{\bullet-}$ charges recombination (75, 76). The expected contribution of the $S_2Q_B^{\bullet-}$ charge recombination to the thermoluminescence glow curve after the second flash, which results from the miss factor (≈ 9%, Table 1), is rather small, and the *traces* shown on Fig. 4*B* can be considered essentially as reflecting the $S_3Q_B^{\bullet-}$ charge recombination (see supplemental data). Fig. 4 shows that the peak temperature of the $S_2Q_B^{\bullet-}$ charge recombination was less affected by the Ca^{2+}/Sr^{2+} and Cl^-/Br^- exchanges than that of the $S_3Q_B^{\bullet-}$ charge recombination, suggesting that the free energy level of $S_2Q_B^{\bullet-}$ is less affected by the substitutions than that of $S_3Q_B^{\bullet-}$. This is consistent with previous studies (22) showing that the reduction in the dark from S_3 to S_2 is three times slower in SrCl-thylakoids when compared with CaCl-thylakoids, whereas the stability of S_2 in the dark is almost unchanged. Fig. 4*B* shows that the peaks arising from the $S_3Q_B^{\bullet-}$ charge recombination in the ion swapped samples were shifted to higher temperatures when compared with that for CaCl-PSII, and the extent of the up-shift

showed the following order: CaCl-PSII < CaBr-PSII < SrCl-PSII < SrBr-PSII (Table 1).

As shown previously (75, 76), the amplitude of the glow curve arising from the charge recombination involving the S_2 state is smaller than that involving the S_3 state. This seems to be an intrinsic property, and a factor of approximately 2 was demonstrated in plant thylakoids (75, 76). In *T. elongatus* the ratio seems to be greater. One possible explanation for this would be a higher $Q_B^{\cdot-}/Q_B$ ratio after the second flash than after the first flash, which would translate into a $Q_B^{\cdot-}/Q_B$ ratio larger than 1 in dark-adapted PSII. This would be at odds with the recent report showing that this ratio is close to or slightly lower than 1 in *T. elongatus* (79), so that other hypotheses should be considered. The larger values found for the peak temperatures after one flash than after two flashes (see also Refs. 58 and 79) indicate that the energy gap between the S_2/S_1 and P_{680}^*/P_{680} couples is higher than that between the S_3/S_2 and P_{680}^*/P_{680} couples. Thus, the higher temperature required to thermally populate P_{680}^* from $S_2Q_B^{\cdot-}$ than from $S_3Q_B^{\cdot-}$ could favor the nonradiative pathways through which charge recombination may occur to the detriment of the radiative pathway.

In principle, the decrease in the energy level of the S_3/S_2 couple can be estimated from the simulation of the thermoluminescence glow curves seen in Fig. 4*B* (also see supplemental data). Nevertheless, the lack of knowledge of the activation energies of the different routes for the charge recombination process, combined with the fact that the Ca^{2+}/Sr^{2+} exchange is known to affect the redox properties of cofactors other than the manganese cluster (*e.g.* it is known to slow down the electron transfer from $Q_A^{\cdot-}$ to Q_B (57)), precludes the accurate determination of the change in the energy level of the $S_3Q_B^{\cdot-}$ state induced by the Ca^{2+}/Sr^{2+} and Cl^-/Br^- exchanges. A qualitative estimate may be obtained, nevertheless, by comparing the shift in T_m observed here with those reported previously in the literature and associated with a known change in the free energy gap. Temperature peaks corresponding to the $S_2Q_B^{\cdot-}$ and $S_3Q_B^{\cdot-}$ glow curves, which differ by ≈8 °C, have been estimated to correspond to a difference in the free energy gap between the S_2 and S_3 state of ≈50–60 meV (80). Recently, a point mutation in the vicinity of Q_A has been found to induce a shift in T_m of 9 °C and a change in free energy of ≈60 meV (81). In the case of the SrBr-PSII, we found an up-shift of T_m by 8 °C, *i.e.* of similar amplitude to those just discussed, so that we estimate the change in free energy associated with the Sr^{2+}/Ca^{2+} and Br^-/Cl^- combined substitution to be ≈50–60 meV. Using the procedure described previously to fit the thermoluminescence glow curves (64), with the assumption that the activation energy value used for the simulations only depends on the enthalpy of the charge recombination, yields a significantly larger downshift (110 meV) for the free energy level of the S_3 state in SrBr-PSII when compared with CaCl-PSII (see supplemental data).

DISCUSSION

The data in Table 1 corresponding to the CaCl and SrCl samples are similar to those obtained earlier with the His_6-tagged PSII (22). The properties of the SrCl samples obtained here in a PSII containing a D1 protein expressed only from the *psbA*$_3$ gene are in agreement with those obtained upon a Ca^{2+}/Sr^{2+} exchange (22) done in the His_6-tagged wild-type strain.

The flash-induced absorption changes measured at 292 nm (Fig. 1) show that the four types of PSII (Ca/Cl, Sr/Cl, Ca/Br, Sr/Br) were fully competent in O_2 evolution. Nevertheless, in those with non-native ion combinations (Sr/Cl, Ca/Br, Sr/Br) the $S_3Tyr_Z^{\cdot}$ to S_0Tyr_Z transition was significantly slowed down (Fig. 2).

Fig. 2 shows complex behavior for the kinetics measured at 292 nm. After the formation of P_{680}^{+}, the change in the tens of nanoseconds time scale corresponds to the pure electron transfer from Tyr_Z to P_{680}^{+}, whereas that in the μs to the hundreds of μs time scale corresponds to the $S_nTyr_ZP_{680}^{+} \leftrightarrow S_nTyr_Z^{+}P_{680} \leftrightarrow S_nTyrZ^{\cdot}P_{680} \leftrightarrow (S_{n+1}Tyr_ZP_{680})' \leftrightarrow S_{n+1}Tyr_ZP_{680}$ equilibria, where the $(S_{n+1}Tyr_ZP_{680})'$ denotes an unrelaxed state (82, 83). A change in the protein relaxation processes is expected to modify one or more of these equilibria. These relaxation processes, occurring in the earlier (ns to tens of μs) time range, can be followed through the reduction kinetics of P_{680}^{+}. In the S_1 state, time-resolved absorption changes at 433 nm showed that none of the exchanges studied here affected P_{680}^{+} reduction in the ns time scale. In contrast, the components present in the μs to the hundreds of μs time range were slowed down by the Ca^{2+}/Sr^{2+} exchange but remained unaffected by the Cl^-/Br^- exchange (not shown, but see supplemental data). This suggests that Ca^{2+}, but not Cl^-, is involved in the relaxation processes associated with (or triggered by) the oxidation of Tyr_Z by P_{680}^{+}.

Fig. 2 shows that the kinetics at 292 nm after the first flash were also modified by the Cl^-/Br^- exchange, in agreement with previous time-resolved studies of the $Tyr_Z^{\cdot}$ decay in Ca-depleted/Sr-reconstituted PSII in all of the S-state transitions (84). As it is widely agreed that none of the S-state transition is kinetically limited by the electron transfer reaction *per se* (7), this indicates that both Ca^{2+} and Cl^- participate in setting the factors that modulate the electron transfer between the Mn_4 cluster and $Tyr_Z^{\cdot}$.

After the third flash, a lag phase can be observed before the absorption decay, which corresponds to the $(S_3Tyr_Z)'$ to $S_0Tyr_Z + O_2$ transition. This lag phase had already been reported (67, 70–72) and was attributed to electrostatically triggered structural rearrangements in the $S_3Tyr_Z^{\cdot}$ states (67), which could involve proton release (72). The data in Fig. 2 show that the duration of the lag phase was significantly increased upon the Ca^{2+}/Sr^{2+} exchange and to a lesser extent upon Cl^-/Br^- exchange. The increase in the lifetime of the intermediate $(S_3Tyr_Z^{\cdot})'$ state in SrBr-PSII could make this sample the material of choice for further characterizations of the events occurring in the lag phase.

We took advantage of the clear slowdown of the O_2 release in SrBr-thylakoids when compared with the SrCl-thylakoids (Fig. 3) in order to study the exchangeability of Cl^- and Br^-. The kinetic consequences of the substitution of bromide for chloride proved to be unaffected by additional washings of the SrBr-thylakoids in a Br^--free, Cl^--containing medium, indicating that under these conditions, the bromide responsible for the slower kinetics is strongly bound and/or occluded. Nevertheless, when the isolated Br^--containing enzyme was incubated

in Cl^--containing buffer in the dark (*i.e.* in the S_1 state) for 6–7 h, the effects of exchange became detectable. The halide exchange kinetics in PSII from the thermophilic cyanobacterium *T. elongatus* thus seem to be comparable with those observed in plant PSII (85).

In plant PSII, the release of Ca^{2+} in PSII lacking some of the extrinsic polypeptides was shown to be very efficient in the S_3 state but hardly occurred (at least under the experimental conditions used) in the S_1 state (86). In addition, the binding of Sr^{2+} in the empty Ca^{2+}-binding site has been shown to require light (28) indicating the likely involvement of the $S_2Tyr_Z^{\bullet}$ state in the binding. These results suggested that in the higher S-state conformational changes occurred making possible the Ca^{2+} (Sr^{2+}) release and Ca^{2+} (Sr^{2+}) binding. Sr-EXAFS spectroscopy performed in SrCl-PSII recently substantiated these conformational changes by providing evidence for modifications in the coordination sphere of the Sr^{2+} ion associated with the successive S-state transitions (34). The S-state dependence of Cl^- release and Cl^- rebinding has been less documented. Nevertheless, it has been shown that reactivation of the S-state cycle in Cl^--depleted PSII by nitrate is more efficient in the higher S-states (43), suggesting that, as for Ca^{2+}, the binding efficiency increases with the S-states.

It should be pointed out that the Ca^{2+}/Sr^{2+} and Cl^-/anion exchange mechanisms discussed in the previous paragraph differ from those involved in biosynthetic exchange. The former involves the structural rearrangement of the Mn_4Ca cluster occurring during the S-state cycle, whereas the latter involves the assembly of the cluster in the photoactivation process (see Ref. 87 for a review). *In vitro* it has been shown that the Sr^{2+} ion is able to substitute for Ca^{2+} in the photoactivation process (87, 88). Biosynthetic exchange studies have shown that this is also the case *in vivo* (Ref. 22 and this work; see also Ref. 30). The demonstration that biosynthetic Cl^-/Br^- exchange is possible is in agreement with *in vitro* photoactivation experiments showing the ability for Br^- to fully substitute for Cl^- (89).

It has been proposed that most experiments in the literature on the role of chloride, including those studying bromide exchange, have been affected by artifacts induced biochemically (51, 52, 90) using chloride depletion procedures. This remains a point of contention in the field, which we will now discuss in the light of the present results, because the strategy followed here eliminated biochemically induced artifacts.

In previous work (52, 85) the binding of Cl^- to PSII was studied with the following protocol. First, the $^{36}Cl^-$ that was incorporated into PSII biosynthetically was found to be fully exchangeable when dialyzed in a $^{35}Cl^-$-containing medium. Second, it was observed that the dialysis of PSII against a Cl^--free medium resulted in only a partial loss of activity (51, 52). Third, the remaining activity arose from all centers turning over at a lower rate. From these observations it was concluded that Cl^- was not required for enzyme turnover (51, 52). This conclusion, however, assumes that all of the Cl^- was released under the conditions used by Lindberg *et al.* (51, 52) for dialysis/washing of PSII in Cl^--free medium (this assumption was not demonstrated experimentally). In short, biosynthetically labeled $^{36}Cl^-$ PSII preparation has not been studied in a Cl^--free medium either in terms of its Cl^- content or in terms of its activity. Admittedly, these would be difficult experiments; however, the point we would like to make is that the conclusion that Cl^- is not required for enzyme turnover remains open to discussion.

Some EXAFS studies suggest a possible Cl^--binding site close to the Mn_4 cluster (91), whereas other EXAFS studies propose that, upon biochemical Cl^-/Br^- exchange, the bromide site is located at a distance greater than 5 Å from the Mn_4 cluster (45). Nevertheless, the chloride depletion protocol (52) used in that work (45) would not have resulted in a full depletion of the PSII-bound chloride as discussed above. Therefore, the bromide site investigated by Haumann *et al.* (45) is not necessarily the one directly associated with the Mn_4 cluster. One way to avoid some of the ambiguities on the number and type of chloride-binding sites would be to use the PSII preparation described in this work.

It is striking that the effects of exchanging Ca^{2+}/Sr^{2+} and Cl^-/Br^- are additive. This might suggest that the physicochemical properties of either Ca^{2+} or Sr^{2+} depend on the presence of either Cl^- or Br^- and vice versa. If this were not the case, it would be more difficult to explain why the Cl^-/Br^- exchange resulted in a further slowdown of the limiting step introduced upon Ca^{2+}/Sr^{2+} exchange. This hypothesis agrees with models for the water oxidation mechanism, which involve the formation of an electrophilic $Mn^V{=}O$ (or Mn^{IV}-oxy radical) and Ca^{2+}-aqua motifs in the S_4 state (see Ref. 37 for a recent review). These models suggest that a chloride ion is close (or bound) to the calcium ion (10, 36, 92). Also, it has been proposed that the lower O_2 activity observed upon Ca^{2+}/Sr^{2+} exchange could be linked to the higher Lewis acidity of aqua-Sr^{2+} *versus* aqua-Ca^{2+} (93). The binding of Br^- to Ca^{2+} and Sr^{2+} could also increase the Lewis acidity of the aqua ion of Ca^{2+} and Sr^{2+}, respectively. This could explain the additive effects of the Cl^-/Br^- and Ca^{2+}/Sr^{2+} exchanges.

Alternatively, the effects of the Cl^-/Br^- exchange investigated here could originate from a more distant halide-binding site. Several long distance effects indeed have been observed already upon Ca^{2+}/Sr^{2+} exchange, such as the decrease of affinity of cytochrome c_{550} followed by manganese release in the absence of betaine,[4] the decrease in the equilibrium constant of $Q_A^{\bullet-}Q_B \leftrightarrow Q_AQ_B^{\bullet-}$ (57), and a change in the environment of the non-heme iron (27). These effects could well be related to the marked effect of Ca^{2+} removal on the redox potential of the $Q_A^{\bullet-}/Q_A$ couple (94). All of these long distance effects could include a modification of the H-bond network around the Mn_4 cluster, which would slow down some of the electron transfer steps. However, although the biosynthetic Ca^{2+}/Sr^{2+} exchange strongly affects several infrared modes in the carboxylate frequency region (30, 32), the biochemical Cl^-/Br^- exchange is reported to be silent in this spectral region (44).

From the thermoluminescence experiment, the decrease in the energy level of the S_3/S_2 couple could be roughly estimated to be 50–110 meV in SrBr-PSII when compared with CaCl-PSII. An implicit hypothesis behind this estimate is that the substitution only affects the energy levels of the S-states. As

[4] A. Boussac, unpublished result.

discussed above, this is certainly an oversimplification, which results in an overestimate of the energy level decrease. Yet, the marked increase in the duration of the lag phase that precedes the oxidation of water and the 6–7-fold slowdown of the water splitting both point to a role of Ca^{2+} and Cl^- in the oxygen production mechanism, raising the issue of the possible correlation between the thermodynamic and kinetics consequences of the substitution.

Clausen and Junge (20) recently reported that water oxidation may be driven backward by increasing the O_2 pressure. They estimated the overall driving force of the $S_3Tyr_Z^{\bullet}/S_4$ to $S_0 + O_2$ transition to be 80 meV (20, 21). In this context, decreasing the available driving force by lowering the free energy level of the $S_3Tyr_Z^{\bullet}$, as in the present case, could affect the overall water splitting process kinetically. However, the kinetics consequences reported here are quite different from those reported from the O_2 back-pressure experiments (20, 21). In the latter case, the amplitude of the millisecond phase associated with water splitting was decreased, and its observed rate was slightly increased. These data could be accounted for by a two-step model involving an intermediate state (*B*) which accumulates under large O_2 pressure and is formed at the expense of $S_3Tyr_Z^{\bullet}/S_4$, It is of note that neither the forward nor the backward rates of the $S_3Tyr_Z^{\bullet}/S_4 \leftrightarrow B$ equilibrium were affected by the increased O_2 pressure. In the present case, the apparent rate constant of the $S_3Tyr_Z^{\bullet}/S_4$ decay is affected, implying that the forward rate constant (and possibly the backward rate as well) of this equilibrium is decreased, so that the efficiency of the chemistry involved is decreased by the Sr^{2+}/Ca^{2+} and/or Br^-/Cl^- substitution (see above for a more detailed discussion of the possible mechanisms).

The lack of changes in the overall amplitude of the ms component indicates, again in contradiction to Clausen and Junge's data (20), that the overall driving force of the $S_3Tyr_Z^{\bullet}/S_4$ to $S_0 + O_2$ transition is not decreased enough to result in a detectable accumulation $S_3Tyr_Z^{\bullet}/S_4$. This is somewhat surprising. Indeed, because the present data point to a decrease in the free energy level of $S_3Tyr_Z^{\bullet}/S_4$ in the modified PSII, such a decrease combined with the shallow driving force of the water splitting reaction (20, 21) should result in the accumulation of a detectable amount of $S_3Tyr_Z^{\bullet}/S_4$. Because of the error bars in our estimate of the change in the free energy level of the S_3 state, this apparent discrepancy may not be irreconcilable. In any case, the SrBr-PSII seems ideally suited for further studies of the effect of O_2 pressure on the water oxidation mechanism.

Acknowledgments—J. Lavergne, P. Sétif, Y. Pushkar, and A. Aukauloo are acknowledged for helpful discussions. Jean-Marc Ducruet is acknowledged for help with thermoluminescence experiments.

REFERENCES

1. Ferreira, K. N., Iverson, T. M., Maghlaoui, K., Barber, J., and Iwata, S. (2004) *Science* **303,** 1831–1838
2. Loll, B., Kern, J., Saenger, W., Zouni, A., and Biesiadka, J. (2005) *Nature* **438,** 1040–1044
3. Diner, B. A., Schlodder, E., Nixon, P. J., Coleman, W. J., Rappaport, F., Lavergne, J., Vermaas, W. F., and Chisholm, D. A. (2001) *Biochemistry* **40,** 9265–9281
4. Groot, M. L., Pawlowicz, N. P., van Wilderen, L. J., Breton, J., van Stokkum, I. H., and van Grondelle, R. (2005) *Proc. Natl. Acad. Sci. U. S., A.* **102,** 13087–13092
5. Holzwarth, A. R., Muller, M. G., Reus, M., Nowaczyk, M., Sander, J., and Rögner, M. (2006) *Proc. Natl. Acad. Sci. U. S. A.* **103,** 6895–6900
6. Rappaport, F., and Diner, B. A. (2007) *Coord. Chem. Rev.* **252,** 259–272
7. Renger, G. (2007) *Photosynth. Res.* **92,** 407–425
8. Kok, B., Forbush, B., and McGloin, M. P. (1970) *Photochem. Photobiol.* **11,** 457–475
9. Yano, J., Kern, J., Sauer, K., Latimer, M. J., Pushkar, Y., Biesiadka, J., Loll, B., Saenger, W., Messinger, J., Zouni, A., and Yachandra, V. K. (2006) *Science* **314,** 821–825
10. McEvoy, J. P., and Brudvig, G. W. (2006) *Chem. Rev.* **106,** 4455–4483
11. Rutherford, A. W., and Boussac, A. (2004) *Science* **303,** 1782–1784
12. Debus, R. J. (2007) *Coord. Chem. Rev.* **252,** 244–258
13. Hillier, W., and Wydrzynski, T. (2004) *Phys. Chem. Chem. Phys.* **6,** 4882–4889
14. Messinger, J. (2004) *Phys. Chem. Chem. Phys.* **6,** 4764–4771
15. Betley, T. A., Surendranath, Y., Childress, M. V., Alliger, G. E., Fu, R., Cummins, C. C., and Nocera, D. G. (2008) *Philos. Trans. R. Soc. Lond. B Biol. Sci.* **263,** 1293–1303
16. Sproviero, E. M., Shinopoulos, K., Gascón, J. A., McEvoy, J. P., Brudvig, G. W., and Batista, V. S. (2008) *Philos. Trans. R. Soc. Lond. B Biol. Sci.* **363,** 1149–1156
17. Siegbahn, P. E. M. (2008) *Philos. Trans. R. Soc. Lond. B Biol. Sci.* **363,** 1221–1228
18. Yano, J., Kern, J., Irrgang, K. D., Latimer, M. J., Bergmann, U., Glatzel, P., Pushkar, Y., Biesiadka, J., Loll, B., Sauer, K., Messinger, J., Zouni, A., and Yachandra, V. K. (2005) *Proc. Natl. Acad. Sci. U. S. A.* **102,** 12047–12052
19. Grabolle, M., Haumann, M., Muller, C., Liebisch, P., and Dau, H. (2006) *J. Biol. Chem.* **281,** 4580–4588
20. Clausen, J., and Junge, W. (2004) *Nature* **430,** 480–483
21. Clausen, J., Junge, W., Dau, H., and Haumann, M. (2005) *Biochemistry* **44,** 12775–12779
22. Boussac, A., Rappaport, F., Carrier, P., Verbavatz, J.-M., Gobin, R., Kirilovsky, D., Rutherford, A. W., and Sugiura, M. (2004) *J. Biol. Chem.* **279,** 22809–22819
23. Ghanotakis, D. F., Babcock, G. T., and Yocum, C. F. (1984) *FEBS Lett.* **167,** 127–130
24. Debus, R. J. (1992) *Biochim. Biophys. Acta* **1102,** 269–352
25. McEvoy, J. P., and Brudvig, G. W. (2004) *Phys. Chem. Chem. Phys.* **6,** 4754–4763
26. Yocum, C. F. (2008) *Coord. Chem. Rev.* **252,** 296–305
27. Boussac, A., Sugiura, M., Lai, T.-L., and Rutherford, A. W. (2008) *Philos. Trans. R. Soc. Lond. B Biol. Sci.* **363,** 1203–1210
28. Boussac, A., and Rutherford, A. W. (1988) *Biochemistry* **27,** 3476–3483
29. Boussac, A., Sugiura, M., Inoue, Y., and Rutherford, A. W. (2000) *Biochemistry* **39,** 13788–13799
30. Strickler, M. A., Walker, L. M., Hillier, W., and Debus, R. J. (2005) *Biochemistry* **44,** 8571–8577
31. Kimura, Y., Hasegawa, K., Yamanari, T., and Ono, T.-A. (2005) *Photosynth. Res.* **84,** 245–250
32. Suzuki, H., Taguchi, Y., Sugiura, M., Boussac, A., and Noguchi, T. (2006) *Biochemistry* **45,** 13454–13464
33. Cinco, R. M., Robblee, J. H., Messinger, J., Fernandez, C., Holman, K. L. M., Sauer, K., and Yachandra, V. K. (2004) *Biochemistry* **43,** 13271–13282
34. Pushkar, Y., Yano, J., Sauer, K., Boussac, A., and Yachandra, V. K. (2008) *Proc. Natl. Acad. Sci. U. S. A.* **105,** 1879–1884
35. Hendry, G., and Wydrzynski, T. (2003) *Biochemistry* **42,** 6209–6217
36. Barber, J., Ferreira, K., Maghlaoui, K., and Iwata, S. (2004) *Phys. Chem. Chem. Phys.* **6,** 4737–4742
37. Meelich, K., Zaleski, C. M., and Pecoraro, V. L. (2008) *Phil. Trans. R. Soc. B.* **363,** 1271–1281
38. Boussac, A., Zimmermann, J.-L., and Rutherford, A. W. (1989) *Biochemistry* **28,** 8984–8989
39. Tang, X. S., Randall, D. W., Force, D. A., Diner, B. A., and Britt, R. D. (1996) *J. Am. Chem. Soc.* **118,** 7638–7639
40. Un, S., Boussac, A., and Sugiura, M. (2007) *Biochemistry* **46,** 3138–3150

41. Homann, P. H. (2002) *Photosynth. Res.* **73,** 169–175
42. Wincencjusz, H., Yocum, C. F., and van Gorkom, H. J. (1999) *Biochemistry* **38,** 3719–3725
43. Wincencjusz, H., Yocum, C. F., and van Gorkom, H. J. (1998) *Biochemistry* **37,** 8595–8604
44. Hasegawa, K., Kimura, Y., and Ono, T.-A. (2002) *Biochemistry* **41,** 13839–13850
45. Haumann, M., Barra, M., Loja, P., Loscher, S., Krivanek, R., Grundmeier, A., Andreasson, L.-E., and Dau, H. (2006) *Biochemistry* **45,** 13101–13107
46. vanVliet, P., and Rutherford, A. W. (1996) *Biochemistry* **35,** 1829–1839
47. Boussac, A., Sétif, P., and Rutherford, A. W. (1992) *Biochemistry* **31,** 1224–1234
48. Boussac, A. (1995) *Chem. Phys.* **194,** 409–418
49. Homann, P. H., and Inoue, Y. (1986) in *Ion Interactions in Energy Transfer Biomembranes* (Papageorgiou, G., Barber, J., and Papa, S., eds) pp. 291–302, Plenum Press, New York
50. Wincencjusz, H., van Gorkom, H. J., and Yocum, C. F. (1997) *Biochemistry* **36,** 3663–3670
51. Lindberg, K., Vänngård, T., and Andréasson, L.-E. (1993) *Photosynth. Res.* **38,** 401–408
52. Lindberg, K., and Andréasson, L.-E. (1996) *Biochemistry* **35,** 14259–14267
53. Ono, T., Zimmermann, J.-L., Inoue, Y., and Rutherford, A. W. (1986) *Biochim. Biophys. Acta* **851,** 193–201
54. Baumgarten, M., Philo, J. S., and Dismukes, G. C. (1990) *Biochemistry* **29,** 10814–10822
55. Zouni, A., Witt, H. T., Kern, J., Fromme, P., Krauss, N., Saenger, W., and Orth, P. (2001) *Nature* **409,** 739–743
56. Kamiya, N., and Shen, J.-R. (2003) *Proc. Natl. Acad. Sci. U. S. A.* **100,** 98–103
57. Kargul, J., Maghlaoui, K., Murray, J. W., Deak, Z., Boussac, A., Rutherford, A. W., Vass, I., and Barber, J. (2007) *Biochim. Biophys. Acta* **1767,** 404–413
58. Sugiura, M., and Inoue, Y. (1999) *Plant Cell Physiol.* **40,** 1219–1231
59. Sugiura, M., Boussac, A., Noguchi, T., and Rappaport, F. (2008) *Biochim. Biophys. Acta*, **1777,** 331–342
60. Kós, P. B., Deák, Z., Cheregi, O., and Vass, I. (2008) *Biochim. Biophys. Acta* **1777,** 74–83
61. Sugiura, M., Rappaport, F., Brettel, K., Noguchi, T., Rutherford, A. W., and Boussac, A. (2004) *Biochemistry* **43,** 13549–13563
62. Béal, D., Rappaport, F., and Joliot, P. (1999) *Rev. Sci. Instrum.* **70,** 202–207
63. Ducruet, J.-M. (2003) *J. Exp. Bot.* **54,** 2419–2430
64. Ducruet, J.-M., and Miranda, T. (1992) *Photosynth. Res.* **33,** 15–24
65. Rappaport, F., Cuni, A., Xiong, L., Sayre, R., and Lavergne, J. (2005) *Biophys. J.* **88,** 1948–1958
66. Styring, S., and Rutherford, A. W. (1987) *Biochemistry* **26,** 2401–2405
67. Rappaport, F., Blanchard-Desce, M., and Lavergne, J. (1994) *Biochim. Biophys. Acta* **1184,** 178–192
68. Lavergne, J. (1991) *Biochim. Biophys. Acta* **1060,** 175–188
69. Lavorel, J. (1978) *J. Theor. Biol.* **57,** 171–185
70. Koike, H., Hanssum, B., Inoue, Y., and Renger, G., (1987) *Biochim. Biophys. Acta* **893,** 524–533
71. Razeghifard, M. R., and Pace, R. J. (1999) *Biochemistry* **38,** 1252–1257
72. Haumann, M., Liebisch, P., Muller, C., Barra, M., Grabolle, M., and Dau, H. (2005) *Science* **310,** 1019–1021
73. Danielsson, R., Albertsson, P.-Å., Mamedov, F., and Styring, S. (2004) *Biochim. Biophys. Acta* **1608,** 53–61
74. Lavorel, J. (1992) *Biochim. Biophys. Acta* **1101,** 33–40
75. Rutherford, A. W., Renger, G., Koike, H., and Inoue, Y. (1984) *Biochim. Biophys. Acta* **767,** 548–556
76. Rutherford, A. W., Crofts, A. R., and Inoue, Y. (1982) *Biochim. Biophys. Acta* **682,** 457–465
77. Devault, D., and Govindjee (1990) *Photosynth. Res.* **24,** 175–181
78. Vass, I. (2003) *Photosynth. Res.* **76,** 303–318
79. Fufezan, C., Zhang, C.-X., Krieger-Liszkay, A., and Rutherford, A. W. (2005) *Biochemistry* **44,** 12780–12789
80. Vos, M. H., van Gorkom, H. J., and van Leeuwen, P. J. (1991) *Biochim. Biophys. Acta* **1056,** 27–39
81. Fufezan, C., Gross, C. M., Sjödin, M., Rutherford, A. W., Krieger-Liszkay, A., and Kirilovsky, D. (2007) *J. Biol. Chem.* **282,** 12492–12502
82. Schilstra, M. J., Rappaport, F., Nugent, J. H. A., Barnett, C. J., and Klug, D. R. (1998) *Biochemistry* **37,** 3974–3981
83. Christen, G., and Renger, G. (1999) *Biochemistry* **38,** 2068–2077
84. Westphal, K. L., Lydakis-Simantiris, N., Cukier, R. I., and Babcock, G. T. (2000) *Biochemistry* **39,** 16220–16229
85. Lindberg, K., Wydrzynski, T., Vänngård, T., and Andréasson, L.-E. (1990) *FEBS Lett.* **264,** 153–155
86. Boussac, A., and Rutherford, A. W. (1988) *FEBS Lett.* **236,** 432–436
87. Ananyev, G. M., Zaltsman, L., Vasko C., and Dismukes, G. C. (2001) *Biochim. Biophys. Acta* **1503,** 52–58
88. Chen, C. G., Kazimir, J., and Cheniae, G. M. (1995) *Biochemistry* **34,** 13511–13526
89. Miyao, M., and Inoue, Y. (1991) *Biochemistry* **30,** 5379–5387
90. Olesen, K., and Andréasson, L.-E. (2003) *Biochemistry* **42,** 2025–2035
91. Fernandez, C., Cinco, R. M., Robblee, J. H., Messinger, J., Pizarro, S. A., Sauer, K., Klein, M. P., and Yachandra, V. K. (1998) in *Photosynthesis: Mechanisms and Effects* (Garab, G., ed) Vol. II, pp. 1399–1402, Kluwer Academic Publishers, Dordrecht
92. Sproviero, E. M., Gascon, J. A., McEvoy, J. P., Brudvig, G. W., and Batista, V. S. (2007) *Curr. Opin. Struct. Biol.* **17,** 173–180
93. Vrettos, J. S., and Brudvig, G. W. (2002) *Philos. Trans. R. Soc. Lond. B Biol. Sci.* **357,** 1395–1405
94. Krieger, A., Rutherford, A. W., and Johnson, G. (1995) *Biochim. Biophys. Acta* **1229,** 193–201